International Journal of ISSI, Vol.2 (2005), No. 2, pp. 24-29

The Effect of Header Geometry on Temperature Distribution in Cold Rolling

Ahmad Saboonchi* and Sayyed Majid Aghili
Department of Mechanical Engineering, Isfahan University of Technology, Isfahan, Iran
Received July 26, 2005; accepted April 9, 2006

Abstract
The objectives in the cold rolling process include improved sheet surface quality and enhanced steel mechanical strength. Given the increasing demand for higher steel surface quality, more rapid production, and thinner steel plates, more attention has been directed toward the parameter of temperature in cold rolling as a means of achieving the above objectives. Due to the friction between work rolls and steel sheet caused during the cold rolling process and because of temperature changes of the work piece during plastic work, a non-uniform temperature distribution results along the work roll axial direction which ultimately leads to improper and undesirable expansion of the work roll along its axis. This, in turn, causes an uneven work roll slide on sheet surface; hence, the uneven and wavy steel surface. In this study, we used headers with a variety of nozzles for cooling the work rolls in order to achieve uniform temperature distribution and thermal expansion of the work roll. In this method, the cooling system is applied to the work roll in such a way that the work roll gains the desired efficiency in terms of both optimized energy consumption and work roll thermal expansion.

Keywords: Heat transfer, Cold-strip rolling, Temperature distribution.

Introduction

The term "rolling" means the set of machining and forming operations on a steel billet to transform it into strips or plates. Generally speaking, the rolling process consists of the passage of a metal work-piece between tworotating work rolls such that the piece is pressed between the work rolls in the plastic state. Rather complicated relationships hold among the elastic transformation of the work roll, the plastic transformation of the metal sheet, heat exchange between the work roll, and the sheet and the ambient environment, governing the final form of the product. A great number of studies have been conducted on these aspects including Bennon [1] who investigated temperature distribution and thermal expansion of the work roll in a 3-D environment using finite difference volume control. He obtained temperature distributions under these conditions together with a constant heat flux in the contact zone and investigated the effects of cooling operations on thermal crown and on work roll thermal expansion. He then developed a sinusoidal model of the conductive heat transfer coefficient and evaluated it in two given coordinates at a constant angle from each other in order to transform the equations into an explicit algebraic form.

*Corresponding author:
Tel: +98-311-3915221 Fax: +98-311-3912628
E-mail address: ahmadsab@cc.iut.ac.ir
Address: Mechanical Engineering Department, Isfahan University of Technology, Isfahan, 84154, IRAN

Tseng [2] employed Generalized Finite Difference (GDF) numerical solution to transform the equations governing the work roll and the plate into algebraic format under steady state conditions while introducing a permutation term for high roll speeds. He obtained temperature distributions over the plastic work on the plate using an irregular mesh and a combination of second order upwind method and a two-dimensional plate model. Ching & Chen [3] first developed a two dimensional model of the work roll in order to obtain the heat flux variations in the contact area and then developed a three-dimensional model of the work roll effecting the thermal source computed in the previous stage using the finite difference volume control in order to estimate the non-steady temperature distributions on the work roll along axial, radial, and circumferential directions. Finally, they obtained the radial expansion of the work roll.

Lin & Lin[4] solved the coupled three-dimensional elastic-plastic finite element equations in order to model the heat source in the plate using the conductance three-dimensional equations. They then developed a three-dimensional model of the work roll and computed heat flux to obtain the temperature distribution in the work roll. Based on the temperature distribution thus obtained, they estimated work roll deformation. Serajzadeh and Mucciardi [5] studied temperature distribution of the work roll in hot slab rolling process using two-dimensional finite element coupled unsteady state heat transfer equations with time-dependent boundary conditions. They modeled the effects of the work roll temperature variations in order to obtain a

more accurate temperature field. They also evaluated the effects of the oils used and of the work roll speed on peak temperature. Saboonchi and Abbaspour [6] obtained the radial and axial work roll temperature distribution under the steady state conditions using the finite difference method through solving the equations governing the work roll in a cylindrical coordinate system neglecting the circumferential conductance under a conductive heat transfer coefficient at the contact area. They evaluated the effects of the spray angle, water pressure, and nozzle type on the thermal crown in the hot rolling process assuming temperature-dependent boundary conditions. The software developed in their work can be run independently from the rolling line.

Methodology

In this study, the work roll and metal temperature distributions are modeled only for the area where plastic work takes place on the strip. Initially, the equations are simplified on the basis of certain accepted assumptions. Along these lines, the circumferential conductance term in the equation governing the work roll in the cylindrical coordinate system is neglected due to the magnitude of the convective term in that direction. Similarly, the conductance term in the rolling direction is neglected in the equation governing the strip. The governing equations are solved for the contact area as equations coupled with the strip-temperature-dependent equation for pressure distribution [7].
On the work roll:

$$\frac{\partial T_r}{\partial t} = \frac{1}{\rho_r C_r}\left[\frac{1}{r}\frac{\partial}{\partial r}\left(K_r r \frac{\partial T_r}{\partial r}\right) + \frac{\partial}{\partial z}\left(K_r \frac{\partial T_r}{\partial z}\right)\right] \quad (1)$$

On the strip:

$$\frac{\partial T}{\partial t} = \frac{1}{\rho_S C_S}\left[\frac{\partial}{\partial y}\left(K_S \frac{\partial T_S}{\partial y}\right) + \frac{\partial}{\partial z}\left(K_S \frac{\partial T_S}{\partial z}\right) + e\right] \quad (2)$$

where, the effect of the convective term is included in the conductance term. At the contact area, a frictional heat source is created between the work roll and the slab due to the presence of slides in that area. The equation governing this can be expressed as follow [2]:

$$K_r\left(\frac{\partial T_r}{\partial n}\right)_r + K_S\left(\frac{\partial T_S}{\partial n}\right)_S + q_f = 0 \quad (3)$$

where,

$$q_f = \mu V_{rel} P \quad (4)$$

Yield stress variations for austenitic steel are shown in Figure 1. Increasing temperature reduces the yield stress [8].

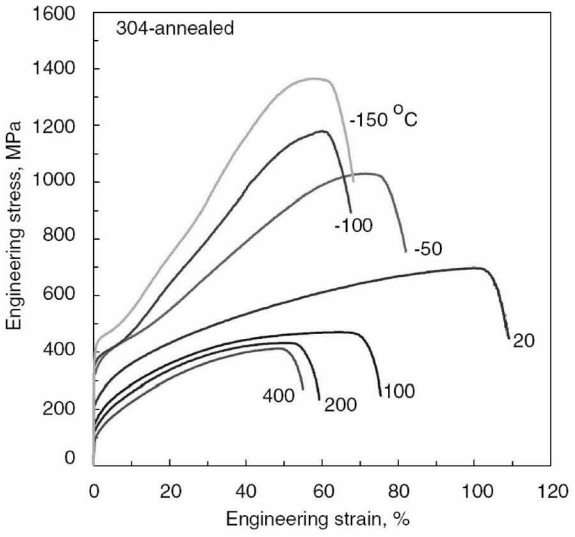

Fig. 1. Yield stress variations in response to temperature and strain changes.

Pressure distribution at the contact area between the work roll and the strip is obtained from Von Karman Equation [9].

$$p\left(\frac{dh}{dx} \pm \mu\right) = \frac{d(h(p - \sigma_C))}{dx} \quad (5)$$

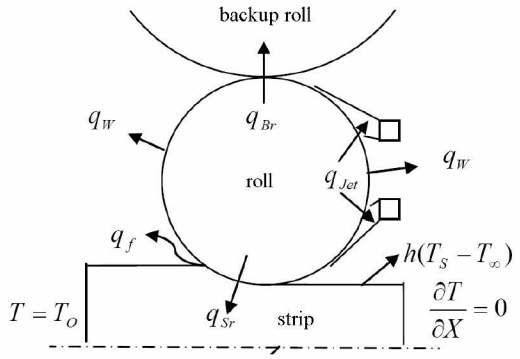

Fig. 2. Boundary conditions on work roll and strip.

The boundary conditions on the work roll head and strip surface are shown in Figure 2. Heat transfer on the work roll is accomplished through air, effluents, the strip, and the fluid sprayed through the jet directly on the work roll. The convective heat transfer coefficient in this area is as follows [6].

$$h_{jet} = h_o C_Q C_P C_\beta C_T C_d \quad (6)$$

where, C_Q, C_p, C_β, C_T, and C_D are volumetric discharge corrective coefficient, pressure, header angle, surface temperature, and nozzle distance from work roll surface, respectively. The geometry of the header is shown in Figure 3 [10,11].

Table 1. Nomenclature.

K	thermal conductivity (W/m K)	r	radial coordinate (m)
T	temperature.	t	time (s)
μ	friction factor	Z	axial coordinate (m)
C	specific heat (J/kg K)	e	heat generation (W/m^3)
C_Q, C_P, C_β, C_T, C_d	correction coefficient		$(\sigma_c \ln \frac{H_i}{H_o})$
$h0$	base heat coefficient for nozzle ($0.12 W/mm^2\ ^\circ C$)	h	*thickness in plastic deformation* (m)
ρ	density (kg/m^3)	V_{rel}	skidding speed with in roll and strip
P	pressure (Pa)	*Subscripts*	
σ_c	yield stress	s	strip
		r	work roll

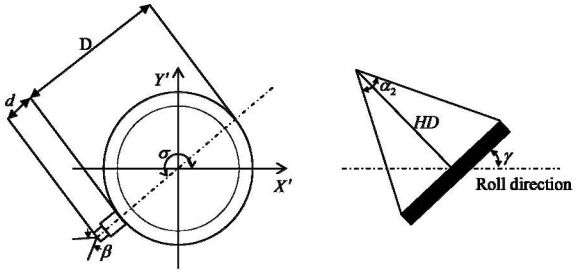

Fig. 3. Geometry of the header on the work roll.

The differential equations governing the work roll and the strip are solved using the finite difference volumetric control. Under these conditions, due to temperature variations along the work roll surface and the strip surface, the mesh for these areas must be finer such that the deeper we move, the larger the mesh spaces will be. The mesh on the strip surface is finer due to the more intense gradients. This situation is clearly seen in Figure 4 for the cross section of the work roll [12].

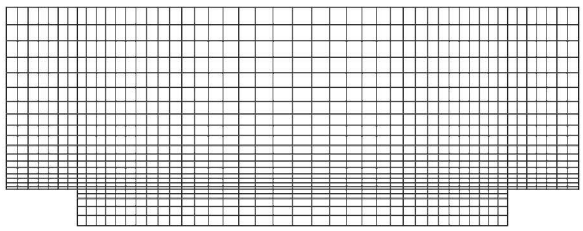

Fig. 4. Meshing of the strip and work roll cross sections.

Results and Discussion

The procedure here takes the following form: the existing boundary conditions are effected for each time range and the equations governing the work roll and the strip are iteratively solved together with the Von Karman time-dependent pressure distribution equation in order to obtain accurate solutions in each section. Outside the contact area, the equation governing the work roll is independently solved. Corrections are made at the boundary and according to the temperature obtained, the mesh for the corrected boundary is iterated enough times until the solutions do not show any change.

The geometry of the work roll and the strip used and the ambient temperature are presented in Table 2 and the thermo-physical properties of the work roll and the strip are presented in Table 3.

The precision and accuracy of the program was first validated against Ref. [13], from which the temperature distribution shown in Figure 5 is obtained where maximum temperature is 131° C. This is comparable to the maximum temperature in Figure 6, which is 125° C whereas the observed temperature was measured at 129°C.

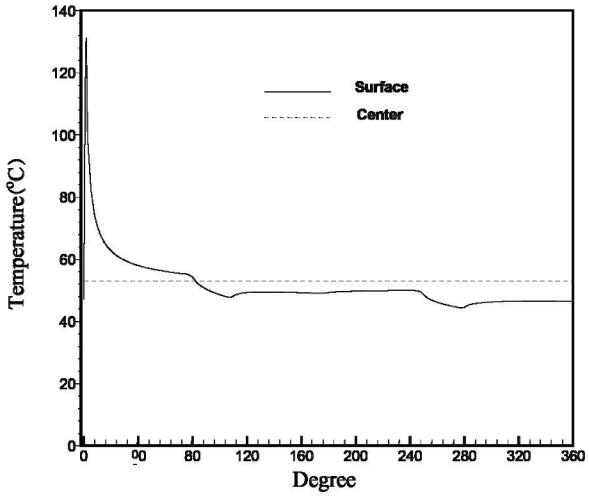

Fig. 5. Temperature distribution on the surface and center of the work roll.

Increased pressure at the header leads to increased fluid discharge. As shown in Figure 7, increased pressure caused the surface temperature to reduce, or, the amount of cooling requirement to increase, which requires the obviously uneconomical increased pumping costs.

As shown in Figure 8, increasing the impact angle around the nozzle axis increases the cooling efficiency due to the increased curve of the work roll exposed to the spray. However, this continues as far as sprays from two consecutive nozzles meet, or

where an overlapping occurs. This causes the pressure on the work roll surface to be neutralized and, thereby, to decrease the heat transfer coefficient to a considerable extent. Increasing the spray angle leads to a larger curve on the work roll surface and a reduced work roll surface temperature. This situation is clearly shown in Figure 9. Therefore, increasing the spray angle obviously increases cooling efficiency. As shown in Figure 10, the rotation of the header around its axis in a manner that the spray on the work roll surface becomes vertical leads to reduced surface temperature and also to increased cooling efficiency. A careful examination of Figure 10 will reveal this situation.

Table 2. Operating conditions.

Strip material	304 Annealed stainless steel	Bearing length	1.02m
Roll material	1078 steel	Strip width	1.12 m
Coolant	Water	Roll diameter	0.5 m
Feed strip thickness	0.15 cm	Back up roll diameter	1.43 m
Output strip thickness	0.114 cm	Bearing diameter	0.38 m
Roll speed	20 rad/s	Feed strip temperature	65.6° C
Roll length	1.52 m	Ambient temperature	25° C

Table 3. Material properties.

Roll density	7837 kg/m^3
Strip density	7871 kg/m^3
Roll conductance [5]	42.28-3.0052*10^{-2}T-1.3509*10^{-5}T^2-4.4298*10^{-8}T^3 (W/m °K)
Strip conductance [5]	59.92-0.0221T-5.4*10^{-5}T^2+4.3*10^{-8}T^3 (W/m^2°K)
Roll specific heat	429.47+0.2575T-5*10^{-5}T^2 (J/kg°K)
Strip specific heat	481 (J/Kg °K)
Yang Modulus of the roll and the back up roll	20.1*10^4 (MPa)
Poisson ratio of the roll and the back up roll	0.296
Roll thermal expansion coefficient	13.0*10^{-6} (1/°C)

T is in degrees centigrade.

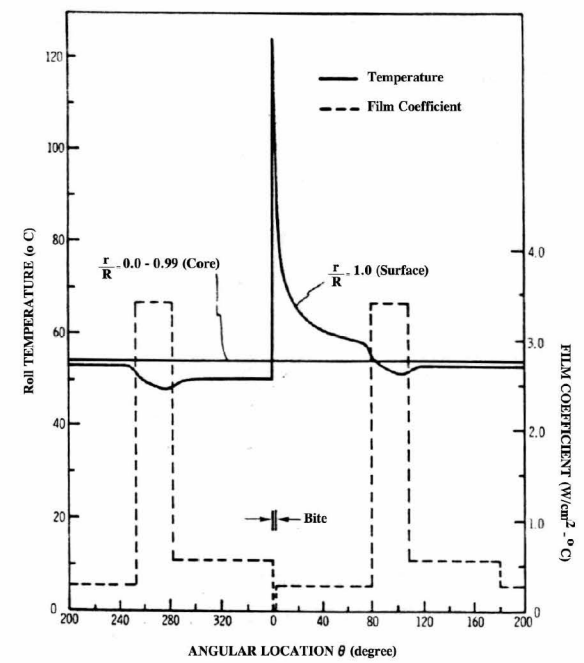

Fig. 6. Temperature distribution on the surface and center of the work roll [5].

In Figure 11, a header 912 mm long with 10 nozzles of the type LECHLER 665004 is mounted on the work roll. The nozzle angle is 20 degrees and the spray angle is 60 degrees. Under these conditions, it is seen that at the work roll edges where it comes in contact with the strip, the temperature increases locally due to direct cooling and as we move toward the center, the temperature distribution gets more even. In Figure 12, the thermal expansion of the work roll is shown with a solid line for these same conditions. Notice that the work roll edges show more variations than in the center due to improper cooling in these areas. This state of affairs causes an undesirable strip profile. The thermal expansion under the conditions where cooling is accomplished through 20 nozzles uniformly deployed on the work roll surface is compared with that obtained under the same conditions but with 10 nozzles in an optimized manner. It is evident from the comparison that increased cooling causes a reduction in the difference in radii of the center and edges of the work roll. This is evidently uneconomical.

In Figure 13, the temperature distribution in the different layers of the strip is shown when the strip is losing contact with the work roll and under conditions where 20 nozzles uniformly deployed on the header have been used. A careful examination of the diagrams reveals that the edges of the strip show a severe temperature drop. This is because the strip is in the process of heat exchange with a work roll that has a thermal crown. This state of affairs leads to dissipating greater heat flux through the strip edges. This heat loss is compensated for by the surface mass but as we move into the depth of the strip, the temperature loss gains a more balanced condition. In

Figure 14, the temperature contour is plotted for the conditions in which the headers have a uniform layout and, like the previous case, 20 nozzles are used for the area on the strip where plastic work takes place. As seen, the temperature on the strip surface is lower than that in its depth because the work roll temperature is low and heat is transferred through surface layers. Therefore, less energy per unit volume of the strip is generated than thermal flux is dissipated and, thus, temperature variation is higher on the surface than it is in the strip depths.

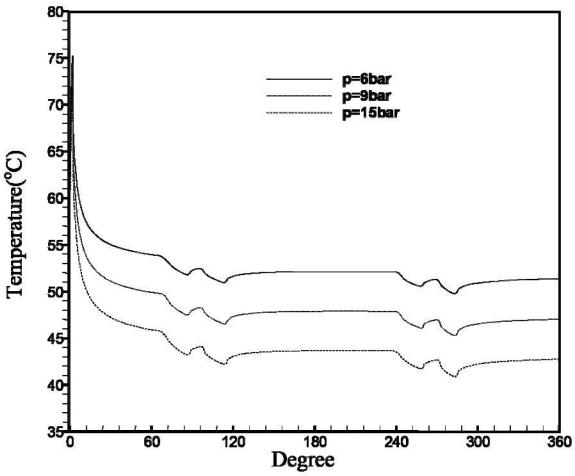

Fig. 7. Work roll surface temperature due to header pressure variations.

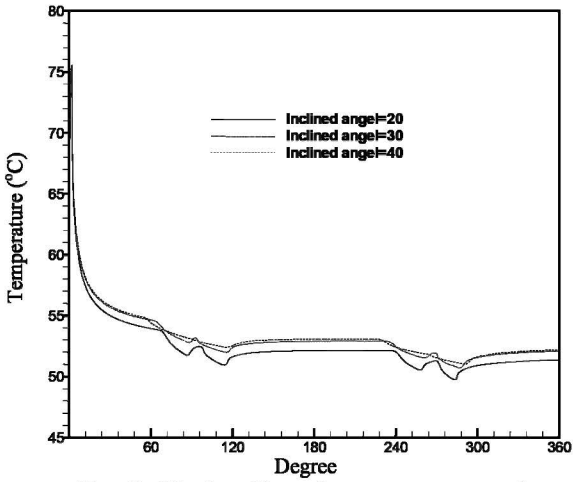

Fig. 8. Work roll surface temperature due to nozzle angle variations.

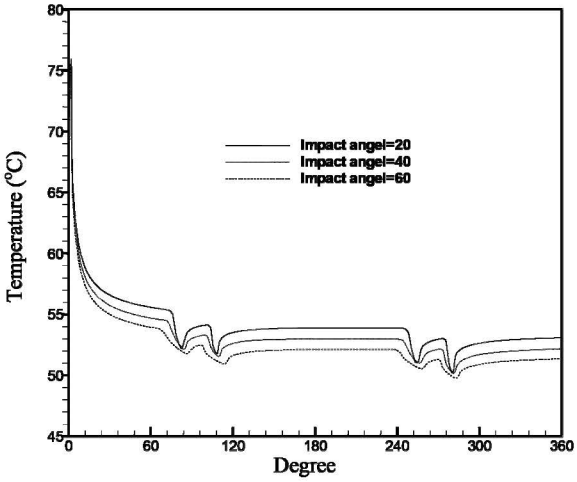

Fig. 9. Work roll surface temperature due to spray angle variations.

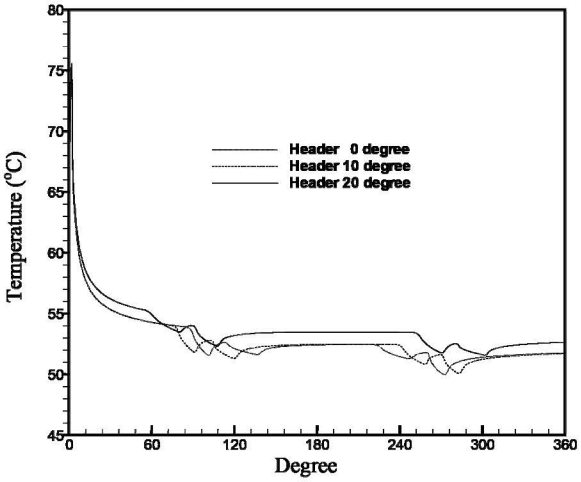

Fig. 10. Work roll surface temperature due to header angle variations.

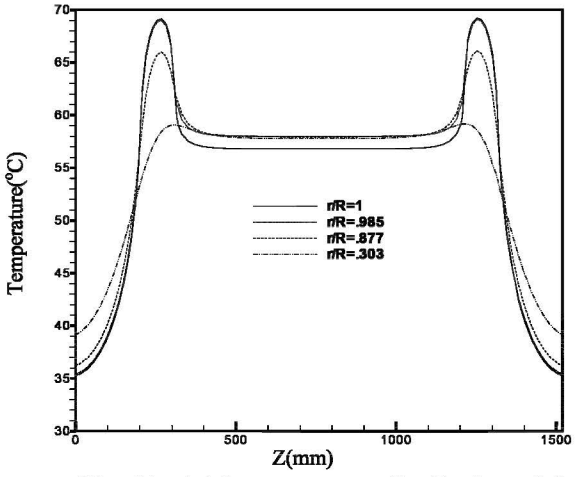

Fig. 11. Axial temperature distribution of the work roll at various radial.

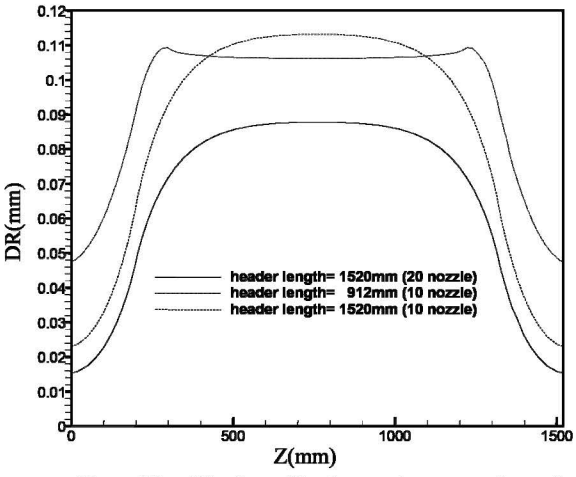

Fig. 12. Work roll thermal expansion for different numbers of nozzles.

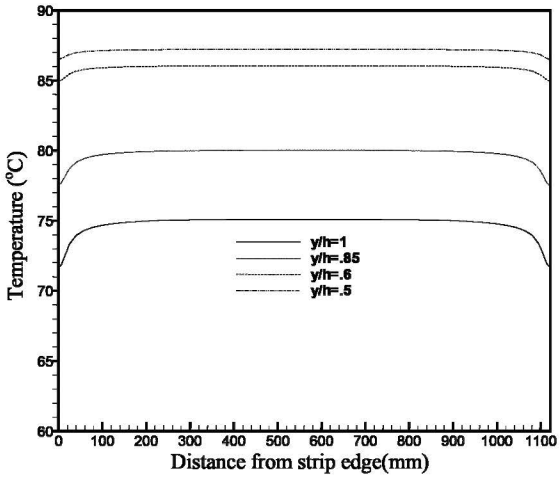

Fig. 13. Strip axial temperature distribution in different layers.

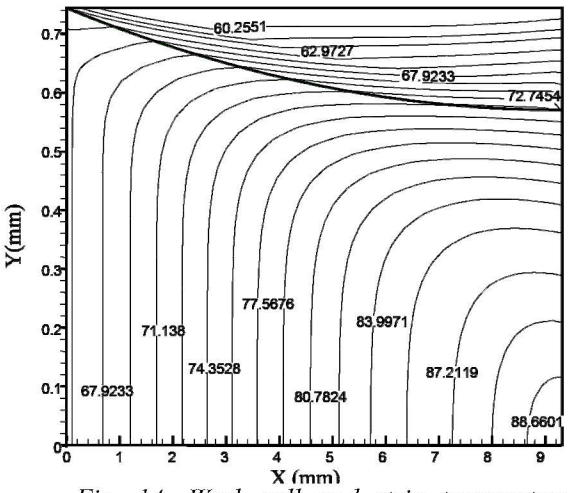

Fig. 14. Work roll and strip temperature contour at the contact area.

Conclusions

In this study, temperature distribution on the work roll is predicted through solving the heat transfer equation using volumetric control based on finite different method. In the solution of these equations, the effects of various factors such as coolant spray on the work roll, cooling by air, and the dependence between temperature and both the work roll and the strip are taken into account. The results obtained can be classified as follows:

1- The most optimal angle for the nozzles (γ) varies between 20 to 30 degrees.

2- The most optimal spray angle (α_2) varies between 50 to 60 degrees.

3- Increasing the number of headers improves the cooling system if the discharge rate and header pressure are kept constant.

4- Increasing pressure greatly helps the uniformity of temperature distribution but it is uneconomical due to increased pumping costs.

5- Collision of the coolant fluid emissions from the nozzles must be avoided as the collision causes a drastic drop in convective heat transfer coefficient on the work roll surface.

6- Header angles must be selected such that the coolant is sprayed on work rolls as directly as possible.

References

[1] W. D. Bennon, ASME. J. Eng. Ind., 107 (1985), 146.

[2] A. A. Tseng, Int. J. for Numer. Meth. Eng., 20 (1984), 1885.

[3] L. Z. Ching, C. C. Chen, J. Mater. Proc. Tech., 49 (1995), 125.

[4] C. Z. Lin, H. V. Lin, J. Mater. Proc. Tech., 70 (1997), 62.

[5] S. Serajzadeh, F. Mucciardi, Model. Simul. Mater. Sci. Eng., 11 (2003) 179.

[6] A. Saboonchi, M. Abbaspour, J. Mater. Proc. Tech., 148 (2004), 35.

[7] A. Saboonchi, M. Abbaspour, Proc. of the Steel Symposium 79, Ahwaz, Iran, (2001), 21.

[8] T. S. Byun, N. Hashimato, K. Farrell, Acta Materialia, 54 (2004) 3889.

[9] W. L. Roberts, New York, Pergamon press, (1969).

[10] V. G. Steden, J. G. M. Tellman, Proc. of the 4th Int. Steel Rolling Conference: the Sci. and Tech. of flat rolling, 1 (1987) 1.

[11] V. B. Ginzburg, Iron and steel Eng., (1997) 38.

[12] J. C. Tannehillm, D. A. Anderson, R. H. Pletcher, Computational fluid mechanics and heat transfer, Second edition, Taylor & Francis publisher, 1997.

[13] A. A. Tsang, F. H. Lin, A. S. Gunderia, D. S. Ni, Metall.Trans. A, 20 (1989) 2306.